face features: bright streaklike markings behind features of positive relief such as crater rims and blocks. These markings appear to be concentrations of fine-grained material (possibly ejecta). It is conceivable that they may be analogous to certain base-surge or ejecta cloud deposits seen on some parts of the lunar surface, but the detailed resemblance is not close.

One of the most exciting results from the October flyby is the evident absence of grooves on Deimos (Fig. 3). From the surface distribution, morphology, and relative age of the grooves on Phobos, Thomas *et al.* (*3*) have concluded that these grooves are surface expressions of modified fractures associated with the formation of Stickney, the largest (10 km in diameter) crater on Phobos. They also showed that the global pattern and old age of the grooves is inconsistent with the tidal-stretching hypothesis proposed by Soter and Harris (*4*).

One possible explanation for the absence of grooves on Deimos is that there is no crater large enough on the surface to have caused such global fracturing. In fact, there is no crater larger than about 3 km on the part of Deimos that has been adequately imaged so far (about half the surface area). A large indentation about 10 km in diameter and 2 km deep does dominate the southern hemisphere; but this indentation does not have a crater-like morphology and may be evidence of the fragmentation of Deimos from a once much larger body.

This large indentation has a strong effect on the principal moments of inertia. For Deimos to be in its stable synchronous rotation about Mars, the indentation must be near one of the poles. In fact, it lies close to the south pole of the satellite.

The Viking data showed Deimos to be within 10 km of the position predicted on the basis of Mariner 9 data (*5*). This prediction error was primarily due to the absence of short-period solar perturbation terms having amplitudes as large as 5 km in the Deimos ephemeris model. The Viking data also suggest that Deimos may be larger than previously believed on the basis of the more limited Mariner 9 data (*6*). Indications are that the volume is between 1200 and 1500 km^3 rather than 1000 km^3. One implication of the increased size is that the average geometric albedo may be lower by about 20 percent than previously believed, about 0.05 to 0.06 rather than about 0.07.

Information on the composition of Deimos remains inconclusive. Various data suggest that, although Deimos probably does not have the same composition as Phobos, it may also consist of some type of carbonaceous material. Tracking data obtained during the October close encounter are currently being processed to derive the mass of Deimos, and additional imagery is being obtained that will make it possible to determine the volume more precisely.

T. C. DUXBURY
Jet Propulsion Laboratory, California Institute of Technology, Pasadena 91103

J. VEVERKA
Laboratory for Planetary Studies, Cornell University, Ithaca, New York 14853

References and Notes

1. J. Veverka and T. C. Duxbury, *J. Geophys. Res.* **82**, 4213 (1977).
2. M. Noland and J. Veverka, *Icarus* **30**, 212 (1977).
3. P. Thomas, J. Veverka, T. Duxbury, *Nature (London)*, in press.
4. S. Soter and A. Harris, *ibid.* **268**, 421 (1977).
5. G. H. Born and T. C. Duxbury, *Celestial Mechan.* **12** (No. 1), 77 (1975).
6. T. C. Duxbury, in *Planetary Satellites*, J. Burns, Ed. (Univ. of Arizona Press, Tucson, 1976), pp. 372–381.
7. We thank Drs. D. Elliot, W. Benton, and L. Shigg of the JPL Image Processing Laboratory for enhancing the Viking television pictures. This report is JPL Planetology Publication No. 314-78-17 and presents the results of one phase of research carried out under contract NAS 7-100 and grant NSG-7156 sponsored by the Viking Program Office and Planetary Geology Program Office, NASA Office of Space Science.

17 February 1978; revised 8 May 1978

Earthquake Swarm Along the San Andreas Fault near Palmdale, Southern California, 1976 to 1977

Abstract. *Between November 1976 and November 1977 a swarm of small earthquakes (local magnitude ≤ 3) occurred on or near the San Andreas fault near Palmdale, California. This swarm was the first observed along this section of the San Andreas since cataloging of instrumental data began in 1932. The activity followed partial subsidence of the 35-centimeter vertical crustal uplift known as the Palmdale bulge along this "locked" section of the San Andreas, which last broke in the great (surface-wave magnitude = 8¼+) 1857 Fort Tejon earthquake. The swarm events exhibit characteristics previously observed for some foreshock sequences, such as tight clustering of hypocenters and time-dependent rotations of stress axes inferred from focal mechanisms. However, because of our present lack of understanding of the processes that precede earthquake faulting, the implications of the swarm for future large earthquakes on the San Andreas fault are unknown.*

Since 1932, when the California Institute of Technology began to catalog instrumental locations of earthquakes in southern California, the section of the San Andreas fault from the Carrizo Plains to Cajon Pass has been seismically quiet (*1*, *2*). This section of the fault is particularly important because of its known capability for rupture in great earthquakes, such as the 1857 Fort Tejon earthquake of surface-wave magnitude (M_s) 8¼+ (*3*). Seismic quiescence was maintained between 1959 and 1974 during a vertical crustal uplift, the Palmdale bulge (*4*), which reached a maximum of 35 cm along the southern half of the 1857 rupture zone near Palmdale, California (Fig. 1).

Between mid-1974 and mid-1976 the uplift partially subsided, with an elevation decrease of 17 cm near Palmdale (*5*). In November 1976 an increase in the number of small earthquakes, of local magnitude (M_L) between 2.0 and 3.0, began in the Palmdale area, near Juniper Hills to the southeast and Lake Hughes to the northwest (Fig. 1). In the year that followed, 1 November 1976 to 1 November 1977, the number of earthquakes with $M_L \geq 2$ was more than an order of magnitude greater than the long-term averages for these two areas (Table 1). This sharp increase in seismicity, however, does not represent a significant increase in strain energy release, since the recent events are all of small magnitude ($M_L \leq 3.0$) and three earthquakes of $M_L \geq 4.0$ occurred in the Juniper Hills and Lake Hughes regions during the period 1932 to 1976 (*1*, *2*). The relocated epicenter for the largest of these (M_L = 5.0, 23 August 1952) lies 2 to 8 km southwest of the San Andreas fault about halfway between Lake Hughes and Juniper Hills (*6*).

The increase in seismicity extends down to $M_L \simeq 0$; this fact has been demonstrated by repeating the extensive 1965 microearthquake surveys of Brune and Allen (*7*), which established the quiescence of this region down to the smallest detectable earthquake thresholds (*8*). Seven movable seismographic trailers were installed to supplement existing coverage in the Lake Hughes area for 38 days in February and March 1976 (*9*). A rate of 1.8 earthquakes per day ($M_L \geq 0$) was determined, compared with 0.1 earthquake per day ($M_L \geq 0$) found between November 1964 and February 1966 by Brune and Allen. The seismographic trailers have been installed near Juniper Hills for more than 1 year, beginning in Nobember 1976, and have recorded about 700 events ($M_L \geq 0$) in 12 months. Essentially no Juniper Hills events were recorded by Brune and Allen's Lake Hughes array, even though it included a high-gain station 30 km from the center of the present activity (*10*). One earthquake of $M_L \geq -1.3$ was recorded by Brune and Allen with an array centered at Littlerock near Juniper Hills during a 23-hour recording period in 1965 (*7*).

The activity at Juniper Hills in 1976 to 1977 can be described as an earthquake swarm, defined by Richter (*11*) as a "long series of large and small shocks with no one outstanding principal event." As far as can be determined, this swarm is the first to occur along the section of the San Andreas fault from Lake Hughes to Juniper Hills since cataloging of instrumental data began in 1932. The uniqueness of this swarm was verified by checking original seismograms from Mount Wilson, a seismographic station 28 km from the 1976–1977 swarm; no swarm activity accompanied previous earthquakes reported in this area. The largest three earthquakes in the swarm occurred on 1 January 1977 ($M_L = 2.8$), 7 March 1977 ($M_L = 3.0$), and 6 September 1977 ($M_L = 2.8$). Activity increased before each of these events, which suggests that if this phenomenon is controlled by the properties of the fault zone, a large earthquake on the same fault might also be preceded by increased activity.

Most earthquakes in the 1976–1977 swarm, including the three largest events, are clustered in a small volume approximately 3 km in maximum dimension (Fig. 1) and at a depth of about 8 km. The locations of these epicenters relative to one another have estimated statistical errors of ± 0.3 km, but the absolute location accuracy may be no better than ± 1 km. The cluster is slightly elongated in a direction perpendicular to the San Andreas and is centered 2 km southwest of the mapped surface trace. Faulting may be along the main San Andreas, or along one of several subparallel faults and lineaments that splay southward from the main fault trace near the cluster location. Among these, the fault showing the largest displacement and longest continuous surface trace is the Punchbowl fault, but since this fault does not clearly break Holocene deposits (*12*) it may no longer be active.

The epicenters of the 1976–1977 earthquakes near Lake Hughes scatter south of the San Andreas fault within the boxed area shown in Fig. 1. The location accuracy in this region is only ± 1 to ± 2.5 km, because there are fewer seismographic stations than at Juniper Hills.

Focal mechanisms for five of the larger events were determined with an azimuthally varying crustal model based on structure studies by Hadley and Kanamori (*13*). Although displacement on the San Andreas fault has been mostly right-lateral strike slip, the mechanisms for the three largest swarm events at Juniper Hills and for the largest event at Lake Hughes show predominantly thrust movement (Fig. 1). The focal mechanism for the first event larger than $M_L = 1$ in the Juniper Hills cluster, however, shows strike slip motion on fault planes trending west-northwest or north-northeast (Fig. 1), suggesting that the swarm was initiated by a slip event on the San Andreas or a conjugate fault trending north-northeast. There is no evidence of an episodic strain change associated with the swarm exceeding a few parts per million (microstrains) at the surface from any of the geodetic networks spanning the San Andreas fault in the Juniper Hills–Lake Hughes area, including a ten-station network in the epicentral area of the swarm (*14*). However, a displacement of up to 10 cm at a depth of 8 km could have occurred without being detected on these networks (*15*).

Table 1. Number of $M_L \geq 2$ earthquakes per year for two regions centered on the San Andreas fault near Palmdale, California (dashed rectangles in Fig. 1). Data from 1953 on are averaged separately since seismographic coverage improved after the 1952 Kern County earthquake ($M_S = 7.7$).

Region	1932 to 1952	1953 to 31 October 1976	1 November 1976 to 1 November 1977
Juniper Hills	0.6	1.0	15.0
Lake Hughes	0.52	0.17	3.0

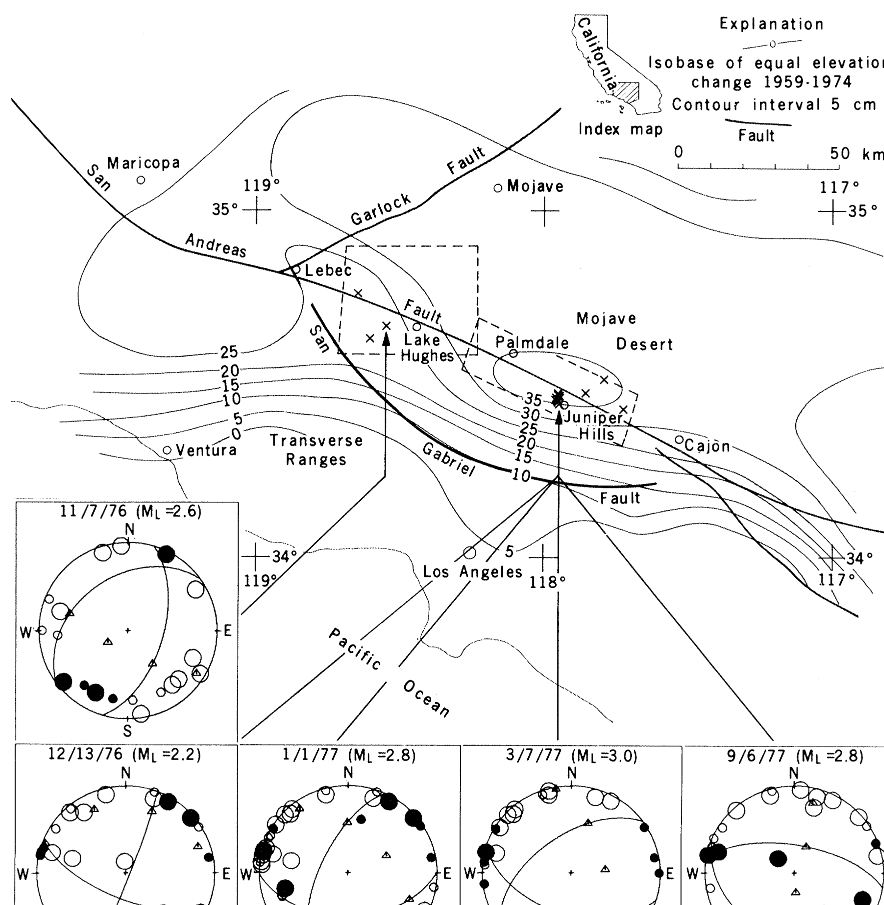

Fig. 1. All earthquakes recorded with magnitude above $M_L \approx 2.0$ within 20 km of the San Andreas fault from Lebec to Cajon from 1 November 1976 to 1 November 1977. The area of maximum uplift between 1959 and 1974 is shown. Dates, magnitudes, and *P*-wave focal mechanism solutions (lower hemisphere) are shown for the largest earthquakes at Juniper Hills and Lake Hughes. Open circles indicate dilatational first motions; closed circles indicate compressional ones. The large circles represent good-quality readings; the small circles, fair-quality readings. Slip vectors, compression axes, and tension axes are shown with triangles.

Table 2. Azimuths of compression axes inferred from fault plane orientations in Fig. 1.

Date	Allowable range	
	Case 1*	Case 2†
7 November 1976	N 58° W ± 14°	N 62° W ± 23°
13 December 1976	N 26° W ± 3°	N 28° W ± 5°
1 January 1977	N 37° W ± 7°	N 35° W ± 17°
7 March 1977	N 11° W ± 5°	N 0° W ± 26°
6 September1977	N 12° E ± 2°	N 18° E ± 7°

*Case 1: best-fit solutions with no additional stations in error. †Case 2: one of the most critical good readings (or two of the most critical fair readings) is in error (*28*).

The focal mechanisms at Juniper Hills are consistent with at least two possible sequences of faulting: (i) movement on southward-dipping, west-northwest–striking fault surfaces with a systematic change in the sense of motion from right-lateral strike slip to combined thrust and right-lateral slip to pure thrust, and (ii) movement on vertical to steeply dipping fault surfaces that change in strike with time from north-northeast to northeast to east-southeast. In the latter case the sense of motion changes from left-lateral strike slip to combined thrust and left-lateral slip to pure thrust, with the orientation of the slip vector remaining approximately the same in all cases. The changes in focal mechanism with time are easily visible in the ratios of the vertical component compressional to shear wave amplitudes (*P*/*SV*) at two nearby stations. The observed ratios, which change by more than an order of magnitude during the swarm, agree with the ratios predicted by the fault plane orientations determined from first-motion diagrams.

The axis of compression inferred from fault plane orientations (Table 2) rotates clockwise from a horizontal northwest orientation nearly parallel to the San Andreas fault to a horizontal north-northeast orientation more consistent with the regional stress field inferred from measurements in situ and other fault plane solutions (*16*). For the three large Juniper Hills thrust events the total rotation observed is 49° ± 9°. This may reflect changes in the local stress field, especially under hypothesis (i), where the fault plane remains approximately the same but the slip vector changes. Under hypothesis (ii), where the slip vector remains approximately the same but the fault plane changes, it is more likely that the local stress field remained the same but the fault planes were dictated by the orientation of preexisting weak zones.

It is clearly of interest to compare the recent Juniper Hills swarm to foreshock sequences that have been studied. Foreshocks to three moderate earthquakes in California—the Galway Lake (M_L = 5.2, 1 June 1975, strike slip), Oroville (M_L = 5.7, 1 August 1975, normal), and Briones Hills (M_L = 4.5, 8 January 1977, strike slip) earthquakes—have been studied (*17*). These foreshocks occurred during time intervals of 3 months, 1 month, and 3 hours, respectively, before the main shocks and were distinguished in all three cases by tight clustering at or near the hypocenter of the impending main shock. The maximum horizontal dimensions of the clusters ranged from 0.5 to 4 km. This type of foreshock behavior has often been noted and may characterize a distinct subset of foreshocks, taken in the broader sense of small earthquakes that precede large ones (*11*, pp. 67–68; *18*). However, it is important to note that tight clustering is also observed in some swarms that are not foreshock sequences, such as the 1970 Danville, California, swarm (*19*).

Rotations in fault plane strikes and inferred axes of compression similar to the rotations observed near Palmdale (Table 2) have occurred during foreshock sequences preceding several moderate-sized thrust events but have not been observed preceding strike slip or normal events. Engdahl and Kisslinger (*20*) report that foreshocks to the Adak Island earthquake (M = 5, 22 February 1976, thrust), which clustered in an area of maximum dimension 5 km containing the main shock, appeared to exhibit an excursion in fault strike of 65° or more from "normal" values during the progress of the sequence, returning to a normal value immediately before the main shock. The strike of the main shock was intermediate between the normal and anomalous strikes. All of the foreshocks were thrusts and occurred over a period of 5 weeks preceding the main shock. Sadovsky *et al.* (*21*) and Nersesov *et al.* (*22*) discussed changes observed in focal mechanisms of small earthquakes before a 14 April 1966 earthquake (M = 5.4, thrust) in the Garm region of the Soviet Union. Earthquakes in a 45 by 15 km region adjacent to the epicenter of 14 April had compression axes that were randomly distributed in azimuth during 1964 but took on a well-defined southeast orientation during 1965. A sudden 90° shift in the compression axes to a northeast preferred orientation took place in late 1965. After the main shock in April 1966, which had an east-northeast compression axis, the compression axes became random in orientation once again. Very similar stress axis rotations were observed before another thrust event in the same region (M = 6.1, 22 March 1969) and also before two M = 4.8 earthquakes in the Naryn Region of the Soviet Union (*23*). Ishida and Kanamori (*24*) studied small earthquakes ($M_L \geq 2.0$) that preceded the San Fernando earthquake (M_L = 6.4, 9 February 1971, thrust), and concluded on the basis of wave-form analysis and seismicity patterns that five events that occurred 0.5 to 2 years before the main event and very near its hypocenter could be considered foreshocks. Although there were not enough data to determine focal mechanisms, *P*-wave first-motion readings at the available stations were nearly identical for these five foreshocks, but were different from the first-motion readings for the main shock and for many of the previous events in this area.

In contrast to these observations, a number of investigators have reported only minor variations in *P*-wave first motions and *P*/*SV* amplitude ratios during foreshock–main shock sequences, indicating that for these events the foreshock mechanisms were similar to each other and to the main shock mechanisms. Fault plane orientations for the foreshocks to the three moderate California earthquakes studied by Lindh *et al.* and discussed above were constant to within 5° to 10° (two cases) and 10° to 20° (one case), as indicated by low scatter in *P*/*SV* amplitude ratios together with *P*-wave first-motion data. The Haicheng earthquake (M_S = 7.3, 4 February 1975, strike slip) and its foreshocks all had similar mechanisms (*25*). These foreshocks (considering only earthquakes located in the hypocentral region of the main shock to be foreshocks) occurred over a period of only 3 days before the main shock. Jones and Molnar (*26*) reported constant ratios of compressional and shear wave amplitudes for foreshocks to three large earthquakes that they studied: one near Luzon, Philippines (M_L = 7.3, 1 August 1968, thrust), one near the Greek island of Crete (M_L = 6.1, 5 December 1968, normal), and one in western Turkey (M_L= 6.6, 28 March 1969, normal). These earthquakes had foreshock sequences with reported durations of 1 day, 2 months, and 1 week, respectively. It should be noted, however, that in the case of the shocks near Crete and in western Turkey the "foreshocks" included shocks with magnitudes as large as 5.9 and 6.2, respectively.

No clear-cut physical explanation has been given for changes in stress axes before strong earthquakes. Brady (*27*) presented theoretical and experimental evidence suggesting that near a concentration of microcracks the axis of compression becomes oriented subparallel to this zone of weakness, but the subsequent events leading to fracture are not well understood.

In summary, a large number of small earthquakes ($M_L \leq 3$) occurred on or near the San Andreas fault near Palmdale, California, between November 1976 and November 1977, constituting an order of magnitude increase in the number of events per year. Although most of the earthquakes clustered tightly in a manner similar to that observed for many foreshock sequences, such clustering is not always diagnostic of foreshocks. The significance of the observed changes in focal mechanism with time is also difficult to evaluate, given the variety of patterns observed in foreshock studies and our incomplete understanding of the processes that precede earthquake faulting. Hence, the implications of the swarm for future large earthquakes on the San Andreas fault are unknown.

K. C. McNally
H. Kanamori
J. C. Pechmann
Seismological Laboratory, Division of Geological and Planetary Sciences, California Institute of Technology, Pasadena 91125

G. Fuis
U.S. Geological Survey, Seismological Laboratory, Division of Geological and Planetary Sciences, California Institute of Technology

References and Notes

1. J. A. Hileman, C. R. Allen, J. M. Nordquist, *Seismicity of the Southern California Region, 1 January 1932 to 31 December 1972* (Seismological Laboratory, California Institute of Technology, Pasadena, 1973).
2. M. E. Friedman, J. H. Whitcomb, C. R. Allen, J. A. Hileman, *Seismicity of the Southern California Region, 1 January 1972 to 31 December 1974* (Seismological Laboratory, California Institute of Technology, Pasadena, 1976).
3. K. E. Sieh, *Bull. Seismol. Soc. Am.*, in press.
4. R. O. Castle, J. P. Church, M. R. Elliott, *Science* **192**, 251 (1976).
5. R. O. Castle, personal communication; J. Bennett, *Calif. Geol.* **30**, 187 (1977); P. Ward, *Summary of a Presentation to the California Seismic Safety Commission* (U.S. Geological Survey, Menlo Park, Calif., 1977).
6. According to C. F. Richter (personal communication), the location of this earthquake and its aftershocks suggest that it was not associated with the San Andreas fault but with a nearby east-northeast–trending fault.
7. J. N. Brune and C. R. Allen, *Bull. Seismol. Soc. Am.* **57**, 277 (1967).
8. Quiescence in the Lake Hughes and Palmdale areas before 1976 was also documented by C. H. Scholz [*U.S. Geol. Surv. Prof. Pap. 733* (1971), pp. 33–37] in a 4½-day microearthquake survey immediately following the 1971 San Fernando earthquake ($M_L = 6.4$).
9. R. L. Carlson, H. Kanamori, K. McNally, *Earthquake Notes* **49**, 30 (Abstr.) (1978).
10. C. R. Allen, personal communication.
11. C. F. Richter, *Elementary Seismology* (Freeman, San Francisco, 1958), p. 71.
12. L. F. Noble, "Geology of the Valyermo Quadrangle and Vicinity, California," *U.S. Geological Survey Geologic Quadrangle Map* (1954); C. R. Allen, personal communication.
13. D. Hadley and H. Kanamori, *Geol. Soc. Am. Bull.* **88**, 1469 (1977); D. Hadley, thesis, California Institute of Technology (1978).
14. J. C. Savage, W. H. Prescott, M. Lisowski, N. King, *Science*, in press.
15. J. C. Savage, personal communication.
16. M. L. Sbar, S. Marshak, T. Engelder, R. Plumb, *Eos* **58**, 1123 (1977); M. Lisowski and J. C. Savage, *Earthquake Notes* **49**, 77 (Abstr.) (1978); C. H. Cramer and J. M. Harrington, *Eos* **58**, 1121 (Abstr.) (1977); J. H. Whitcomb, C. R. Allen, J. D. Garmany, J. A. Hileman, *Rev. Geophys. Space Phys.* **11**, 693 (1973); J. C. Pechmann, unpublished fault plane solutions.
17. A. Lindh, G. Fuis, C. Mantis, *Science* **201**, 56 (1978); B. Bolt, J. Stifler, R. Uhrhammer, *Bull. Seismol. Soc. Am.* **67**, 1555 (1977).
18. T. V. McEvilly, W. M. Bakun, K. B. Casaday, *Bull. Seismol. Soc. Am.* **57**, 1221 (1967); C. R. Allen and J. M. Nordquist, *U.S. Geol. Surv. Prof. Pap. 787* (1972), pp. 16–23; K. C. McNally, *Bull. Seismol. Soc. Am.*, in press; M. Ishida and H. Kanamori, *Geophys. Res. Lett.* **4**, 345 (1977).
19. W. H. K. Lee, M. S. Eaton, E. E. Brabb, *Bull. Seismol. Soc. Am.* **61**, 1771 (1971).
20. E. R. Engdahl and C. Kisslinger, *J. Phys. Earth*, in press.
21. M. A. Sadovsky *et al.*, *Tectonophysics* **14**, 295 (1972).
22. I. L. Nersesov, A. A. Lukk, V. S. Ponomarev, T. G. Rautian, B. G. Rulev, A. N. Semenov, I. G. Simbireva, in *Earthquake Precursors*, M. A. Sadovsky, I. L. Nersesov, L. A. Latynina, Eds. (Soviet Academy of Sciences, Moscow, 1973), D. B. Vitaliano, Transl. (U.S. Geological Survey, Reston, Va., 1974).
23. I. G. Simbireva, in *Experimental Seismology*, M. A. Sadovsky, Ed. (Science Press, Moscow, 1971), D. B. Vitaliano, Transl. (U.S. Geological Survey, Reston, Va., 1973).
24. M. Ishida and H. Kanamori, *Bull. Seismol. Soc. Am.*, in press.
25. Haicheng Earthquake Study Delegation, *Eos* **58**, 236 (1977); Jin Yan, Zhao Yi, Chen Yong, Yan Jai-Quan, Zhour Yu-ru, *Ti Ch'iu Wu Li Hsueh Pao* (*Acta Geophys. Sin.*) **19**, 156 (1976); P. M. Muller, Ed., *Proceedings of the Lectures by the Seismological Delegation of the People's Republic of China*, M. Ohnuki, Kwok Maw Ong, Chia-Chun Chao, Transl. (Jet Propulsion Laboratory, California Institute of Technology, Pasadena, 1976).
26. L. Jones and P. Molnar, *Eos* **58**, 1195 (Abstr.) (1977).
27. B. T. Brady, *Pure Appl. Geophys.* **112**, 701 (1974).
28. The error bars were computed by using J. Whitcomb's computer program FOCPLT, which computes the number of stations in error for all possible solutions spaced at approximately 5° intervals, using a 3° taper near the nodal plane [J. H. Whitcomb, thesis, California Institute of Technology (1973)].
29. We thank D. Anderson, C. Allen, K. Sieh, A. Barrows, C. Johnson, J. Whitcomb, J. Rudnicki, C. Richter, R. Castle, V. Taylor Lehner, D. Tanner, M. French, and L. Blayney for helpful suggestions and technical assistance. This work was supported by grant 14-08-0001-16711 from the U.S. Geological Survey. Contribution No. 3040, Division of Geological and Planetary Sciences, California Institute of Technology.

8 May 1978; revised 10 July 1978

Estrogen-Binding Sites in Endothelial Cell Cultures

Abstract. *The cytosol extracted from a vascular endothelial cell line binds [^{3}H]estradiol with high affinity and a high degree of specificity. In contrast, in experiments performed with cytosol labeled in the intact cell, progesterone and, to a smaller extent, testosterone gave an apparent inhibition of estradiol binding. These data support the concept that ovarian hormones may influence the role of the endothelium in various physiological and pathophysiological conditions.*

The low incidence of atherosclerosis in premenopausal women has suggested that sex-linked factors may have a role in the prevention of this vascular disorder. After menopause, the difference between sexes in the susceptibility to the disease tends to diminish. Similarly, ovariectomized women exhibit a degree of atherosclerosis closer to that of men than healthy women (*1*). Among the changes associated with the loss of ovarian function, variations in the type and amount of circulating blood lipids have been reported (*2*). The possibility that local vascular events that are under the influence of ovarian hormones play a role in the development of the atherosclerotic lesion has not been sufficiently explored. Since an impairment of the endothelial function may be responsible for the changes in structure and composition of the subendothelial intima that are observed during the development of the atherosclerotic plaque, a precise definition of the metabolic characteristics of the endothelium is of particular importance. Experiments performed with intimal tissue may not lead to a correct analysis of the functional activities of the endothelial lining of the artery because, aside from the difficulty of obtaining a pure intimal layer, cells other than endothelial, presumably smooth muscle cells, are present in the intima itself. The availability of an endothelial cell line (*3*) and of a subendothelial cell line derived from the intima of male rabbit aorta has made it possible for us to ascertain whether any of the cell types present in the intima are potentially capable of responding to estrogens. Our results indicate that endothelial cell cultures possess estrogen receptors whereas the other cell line of intimal derivation does not.

The subendothelial cell line used for these studies was obtained by removing first the endothelial lining of the artery as indicated elsewhere (*3*). The cells released into the lumen of the vessel during a second incubation period with enzyme

0036-8075/78/0901-0817$00.50/0